Equilibrium and kinetic analysis of Phosphorus adsorption from aqueous solution using waste alum sludge

A.O. Babatunde* and Y.Q. Zhao

Centre for Water Resources Research, School of Architecture, Landscape and Civil Engineering,

Newstead Building, University College Dublin, Belfield, Dublin 4, Ireland

---

*Corresponding author: Tel: +353-1-7163209, Fax: +353-1-7163297

E-mail: akintunde.babatunde@ucd.ie

Abstract

Excess phosphorus (P) in wastewaters promotes eutrophication in receiving waterways. A cost-effective method such as use of novel low-cost adsorbents for its adsorptive removal would significantly reduce such impacts. Using batch experiments, the intrinsic dynamics of P adsorption by waste alum sludge (an inevitable by-product of drinking water treatment plants) was examined. Different models of adsorption were used to describe equilibrium and kinetic data, calculate rate constants and determine the adsorption capacity. Results indicate that the intraparticle rate constant increased from 0.0075 mg g^{-1} min^{-1} at 5 mg L^{-1} to 0.1795 mg g^{-1} min^{-1} at 60 mg L^{-1} indicating that more phosphate is adsorbed per gram.min at higher P concentration. Further analyses indicate involvement of film and particle diffusion mechanisms as rate controlling steps at lower and higher concentrations respectively. Mass transfer coefficient obtained ranged from 1.7×10^{-6} to 1.8×10^{-8} indicating a rapid transportation of phosphate molecules onto the alum sludge. These results further demonstrates that alum sludge – hitherto thought of as undesirable waste, can be used as novel adsorbent for P removal from wastewater through various applications, thus offsetting a portion of the disposal costs while at the same time improving water quality in sensitive watersheds.

Keywords Adsorption capacity, adsorption kinetics, adsorption models, alum sludge, phosphorus

1. Introduction

Phosphorus (P) is an essential, often limiting, nutrient for growth of organisms in most ecosystems and it is also a very important material for many industries. However, its extensive industrial use inevitably results in large amounts of P-bearing wastes which are usually discharged into municipal and industrial effluent streams. The need for efficient removal of P from wastewaters before discharge into watercourses is well understood. It is well known that the release of P from wastewaters into watercourses can cause severe pollution problems, such as eutrophication which frequently results in algal blooms, fish kills and loss of water resources. The cost of eutrophication to the UK water industry is estimated at > £15M per annum [1], while it is reported that about 30% of the Irish river channel length is polluted mainly from eutrophication [2]. Thus, the continued search for cost-effective methods for P removal remains a high priority in order to control and remedy eutrophication problems and maintain a sustainable green environment for the future.

In recent times, P removal using waste materials or by-products as novel adsorbents has been gaining increased attention. Reviews on such materials which include slag materials, burnt oil shale and ashes from the thermal incineration industry have been published [3, 4]. Another by-product which is a promising low-cost adsorbent for P removal from wastewaters is waste alum sludge. Alum sludge is a by-product of water treatment plants that use aluminium salts as primary coagulant and it is the most widely generated water treatment residual/sludge worldwide [5]. Alum sludge usually contains colloidal alum hydroxides which are often an amorphous species. These generally have larger surface area and greater reactivity toward anion adsorption than the corresponding crystalline mineral phases. Due to

the relative abundance of aluminium in the alum sludge and the high reactivity, they possess a high capacity for phosphorus removal through adsorption [5].

Compared to other by-products that have been considered as adsorbent for P removal, alum sludge possesses a distinct advantage because it is an easily and freely available by-product in towns, cities and metropolis regions worldwide that utilize surface waters as a drinking water source, and therefore, its availability is guaranteed. A number of researches have been conducted to demonstrate the potential use of alum sludge as adsorbent for P removal while its use as a P removing substrate in constructed and engineered wetland systems is also being actively promoted and demonstrated [5, 6, 7, 8, 9, 10]. However, most of these studies have been limited to the characterization and the determination of the P adsorption capacity of the alum sludge. In this study, the intrinsic dynamics of P adsorption from aqueous solution by the alum sludge is investigated. Such a study is important in understanding the dynamics of P adsorption by the alum sludge and facilitating its efficient use for P removal in practise.

2 Materials and methods

2.1 P-adsorption experiments

Dewatered alum sludge cakes were collected from the largest water treatment plant in Ireland, located in Co. Kildare, Ireland. The plant uses aluminium sulphate for reservoir water flocculation. The alum sludge cakes were air-dried and ground to pass a 2-mm mesh sieve prior to being used. The physico-chemical characteristics, the equilibrium time and optimal dosage for P adsorption by the alum sludge have been determined and reported [6]. Regarding the metal composition of the dewatered alum sludge, the results show that the relative proportion of aluminium, iron, arsenic, lead, titanium and zinc were 42.67, 3.34, 0.034, 0.005, 0.099 and 0.03 mg g^{-1} respectively (metals analysed were based on their presence in the alum

sludge from). It should however be noted that except for aluminium, the levels of most other metals in the alum sludge especially lead and zinc, are below their typical levels in uncontaminated soils [6]. Furthermore, a 42-week leaching analysis from a pilot field-scale study utilizing the alum sludge shows that although mainly aluminium leaching was observed in the first three weeks of operation, effluents concentrations of both total and soluble Al were all below the general regulatory guideline limit of 0.2 mg L^{-1} for drinking water quality standard and effluent discharge [unpublished results]. It was therefore concluded that concerns about the leaching of aluminium or other metals should not restrict its use although periodical monitoring is recommended. Regarding the morphological structure of the alum sludge, X-ray diffraction analysis reveals no sharp diffraction characteristic, while SEM observation of the alum sludge shown in Figure 1 did not reveal any classical well-crystalline appearance on its surface suggesting that the alum sludge is amorphous.

A contact time of 48 hours and an optimal dosage of 10 g L^{-1} were determined. To obtain equilibrium data for determining the P adsorption capacity and affecting factors, one gram of the alum sludge was equilibrated with 100 ml of P solution with concentrations ranging from 0 to 360 mg P L^{-1} for 48 hours at three different pH levels (4, 7, 9). After the set time (48 hours), the mixture was withdrawn and filtered using a 0.45 μm Millipore membrane filter and analysed for residual P using a HACH DR/2400 spectrophotometer according to its standard operating procedures. The amount of P adsorbed by the alum sludge from the solution at equilibrium, q_e in mg g^{-1}, was computed using Eq.1.

$$q_e = \frac{(C_o - C_e)V}{m} \qquad \text{Eq. 1}$$

where C_o and C_e (both in mg L^{-1}) are the initial and final P concentrations at equilibrium respectively. Data obtained were fitted to linearised forms of Langmiur, Freundlich, Dubinin-Radushkevich (D-R), Temkin, Frumkin and Harkins–Jura adsorption isotherm models in order to determine the adsorption parameters.

[INSERT FIG. 1 HERE]

The description of these adsorption isotherm models is widely available in scientific texts and literature and will not be repeated here. However, the adsorption isotherm equations, their corresponding linear forms and the parameters obtained from linearization are summarized and presented in Table 1, section 3.1.

2.2 Kinetics of P- adsorption by the alum sludge

To examine the kinetics of the P adsorption process, the batch technique was also used. A number of 250 ml bottles were filled with 100 ml of P solutions at four different P concentrations (5, 15, 30, and 60 mg L^{-1}), and 1 g of the alum sludge was added to each bottle. The mixture was then agitated at 200 rpm on the rotary shaker. At predecided times, the mixtures were withdrawn, filtered and analysed for P uptake using Eq. 1. The kinetic data were then analysed as discussed below.

2.2.1 Adsorption rate constant

The kinetics of P adsorption process by the alum sludge was examined by the pseudo-first-order equation (Eq. 2): [11]

$$\frac{dq_t}{dt} = K_1(q_e - q_t) \qquad \text{Eq. 2}$$

where q_t is the amount of adsorbate adsorbed at time t (mg g^{-1}), K_1 is the pseudo-first-order rate constant (min^{-1}) and t the contact time (mins). Solving the equation, it can be written as

$$\log(q_e - q_t) = \log q_e - \frac{K_1}{2.303}t \qquad \text{Eq. 3}$$

The kinetic data were also fitted to the pseudo-second-order equation which has the form: [12]

$$\frac{dq_t}{dt} = K_2(q_e - q_t)^2 \quad \text{Eq. 4}$$

where k_2 is the pseudo-second-order rate constant (g mg^{-1} min^{-1}). Solving the equation, it can be written as

$$\frac{t}{q_t} = \frac{1}{k_2 q_e^2} + \left(\frac{1}{q_e}\right)t \quad \text{Eq. 5}$$

The intraparticle diffusion model was also used [13, 14]

$$q = k_d t^{1/2} \quad \text{Eq. 6}$$

where k_d (mg g^{-1} $min^{-1/2}$) is the rate constant for intraparticle diffusion. The initial rates of intraparticle diffusion can be obtained by linearization of Eq.6. The values were further supported by calculating the intraparticle diffusion coefficient $\overline{D}$ (cm^2 s^{-1}) using Eq. 7 [15]

$$\overline{D} = 0.03r^2/t_{1/2} \quad \text{Eq. 7}$$

where $t_{1/2}$ (min) is the time for half of the adsorption and r is the average particle radius of the adsorbent particles.

2.2.2 Mass transfer

To further examine the kinetics of P adsorption and calculate the mass transfer coefficient β_L, experimental kinetic data were fitted to a mass transfer model [16]

$$\ln\left[\frac{C_t}{C_o} - \frac{1}{1+mk}\right] = \ln\left[\frac{mk}{1+mk}\right] - \left[\frac{1+mk}{mk}\right]\beta_L S_s t \quad \text{Eq. 8}$$

where C_t and C_o (both in mg L^{-1}) are the respective concentrations of P in solution at time t and zero and k (in L g^{-1}) is a constant obtainable by multiplying the Langmuir constants Q_m and b. m (g L^{-1}) and S_s (cm^{-1}) are, respectively, the mass and outer surface area of the adsorbent particles per unit volume of particle free solution and β_L (cm^{-1}) is the mass transfer coefficient. The values of m and S_s are calculated using the following equations:

$$m = \frac{W}{V} \quad \text{Eq. 9}$$

$$S_s = \frac{6m}{(1-\varepsilon_P)d_P\rho_P} \quad \text{Eq. 10}$$

where W is the weight of the adsorbent (g), V is the volume of particle free adsorbate solution (L), d_p is the particle diameter (cm), ρ_P is the density of the adsorbent (g/cm), and ε_P is the porosity of the adsorbent particle. β_L was determined by linearizing Eq. 8.

2.2.3 Rate expression

For the proper understanding of the experimental data, it is necessary to identify the rate controlling step governing the overall adsorption process. Boyd et al. [17] and Reichenberg [18] gave the expression of Eq. 11

$$F = 1 - \frac{6}{\pi^2}\sum_{1}^{\infty}\left(\frac{1}{n^2}\right)\exp\left(-n^2 B_t\right) \quad \text{Eq. 11}$$

Where F is the fractional attainment of equilibrium at time‘t’ and is obtained from Eq. 12 and n is Freundlich constant of the on going adsorption process.

$$F = \frac{Q_t}{Q_\infty} \quad \text{Eq. 12}$$

where Q_t and Q_∞ are the amount of uptake at time t and equilibrium, respectively. For every value of F, corresponding pre-calculated value of B_t was derived from the Reichenberg’s table [17]. Thereafter, plots of time versus B_t were obtained at different initial P concentrations. The linearity of B_t versus t is employed to distinguish between the film and particle controlled mechanism [19]. To evaluate the data, the slopes of the straight line plots obtained at the different concentrations were taken as B, the time constant, and this was subsequently used for the evaluation of the values of Di using Eq. 13

$$D_i = \frac{Br_o^2}{\pi^2} \qquad \text{Eq. 13}$$

where D_i is the effective diffusion coefficient of adsorbate in adsorbent phases, r_o is the radius of the adsorbent particle assumed to be spherical and n is an integer.

3 Results and discussion

3.1 *Determination of adsorption isotherm constant and maximum adsorption capacity*

The fitting of the experimental data to the linear forms of the six adsorption isotherm is shown in Fig. 2a, b, c, d, e and f for Langmiur, Freundlich, D-R, Temkin, Frumkin and Harkins–Jura models respectively. The parameters obtained from the linearization alongside the model equations and their linear forms are shown in Table 1. The results of the fitting of the experimental data to the Langmuir and Freundlich models have been discussed elsewhere [6] and would only be mentioned here briefly. R^2 were found to be highest for the Langmuir plots ranging from 0.97 to 0.98 indicating its best fit. The Freundlich, D-R, Temkin and Frumkin plots also gave high R^2 values ranging from 0.81 to 0.97 with the exception of D-R plot at pH 9 which gave a R^2 value of 0.65. However, the H-J model was not analysed further since it appears to be poorly fitted (R^2:0.61 to 0.69).

[INSERT FIG. 2 HERE]

[INSERT TABLE 1 HERE]

The maximum adsorption capacity evaluated from the Langmuir isotherm plot was determined to be 31.9 mg P g^{-1} at pH 4 and the value of the adsorption capacity decreased with an increase in pH from 4 to 9. Previous investigations indicate that the adsorption capacity varied from 3.3 mg P g^{-1} to 23.9 mg P g^{-1} depending on the alum sludge and test conditions such as initial concentration, pH and age of the alum sludge [20, 21]. In

comparison to the maximum adsorption capacity of other materials cited in literature as determined from the linearised plot of the Langmuir model [9, 10, 22], the alum sludge used in this study can be seen to have a significant and comparable P adsorption capacity. For instance, Sakadevan and Bavor [22] used the Langmuir model to determine the maximum P adsorption capacity of soils, slags and zeolites and obtained a range of values from 0.93 to 44.3 mg P g^{-1}. Similarly, in two separate studies using water treatment plant residual for P adsorption, Kim et al. [9] and Ippolito et al. [10] calculated removal capacites of 25 mg P g^{-1} and 12.5 mg P g^{-1} respectively using the Langmuir model. Thus, with P adsorption capacity values ranging from 10.2 mg P g^{-1} to 31.9 mg P g^{-1}, the alum sludge used in this study can be seen to have a reasonable and high P adsorption capacity as compared to the capacity of other adsorbents reported in literature.

The D-R plot of log q_e vs ε^2 at the different pH is shown in Fig. 2c and the constants parameters determined are also listed in Table 1. The mean adsorption energy, *E*, which gives information about chemical and physical adsorption was found to be in the range 17.7 to 21.3 KJ mol^{-1}. This is bigger than the energy range of adsorption reaction (8-16 KJ mol^{-1}) [23], and thus the adsorption of P onto the dewatered alum sludge cakes may also involve chemical adsorption. The Temkin plot (Fig. 2d) and the parameters obtained listed in Table 1 indicate that the constant B_1 which represents the heat of adsorption decreased with an increase in pH. This may also suggest an increase in adsorption activity at the low pH. The positive values of constant 'a' in the Fumkin model indicate that there is attractive interaction between the adsorbed species [23], i.e. the phosphate molecules and the alum sludge.

3.2 Adsorption rate constant studies

The experimental data were fitted to both the first and second order adsorption models with correlation coefficients of R^2 = 0.92-0.97 and R^2 = 0.99 obtained respectively (Fig. 3a,

b). Although high correlation coefficients were obtained from the fitting of the data to the first and second-order models, several authors have shown that the adsorption of P fits better with the second-order-adsorption model than the first order [24, 25, 26]. From the slopes derived from the straight line plot of the first and second order adsorption model, respective values of the rate constants of adsorption, k_1 and k_2 respectively, at different initial P concentration were determined.

Values of the rate constants of adsorption at P concentrations of 5, 15, 30 and 60 mg L^{-1} were determined to be 5.0×10^{-2}, 2.0×10^{-2}, 1.4×10^{-2} and 1.1×10^{-2} min^{-1}, and 8.3×10^{-1}, 1.3×10^{-1}, 0.5×10^{-1} and 0.2×10^{-1} g mg^{-1} min^{-1} for the first and second order models respectively. Similarly, the q_e values were determined to be 0.11, 0.44, 1.06 and 2.30, and 0.51, 1.45, 2.54 and 4.47 mg g^{-1} for first and second order models respectively. In both cases, the rate constants were found to decrease with increasing initial P concentration while q_e values increased with increase in initial P concentration. This indicates that the contact time necessary to achieve equilibrium might be affected by the initial P concentration, with more time being necessary to reach equilibrium at the higher values of the initial P concentration. However, the P uptake increases with increase in initial P concentration. This same trend was reported for P adsorption by Namasivayam and Sangeetha [24]. In this study, at an initial P concentration of 30 mg P L^{-1}, values of 0.014 min^{-1} and 0.05 g $mg^{-1}min^{-1}$ were obtained for k_1 and k_2 respectively. At the same initial P concentration of 30 mg P L^{-1}, Ozacar [27] and Namasivayam and Sangeetha [24] reported values of 0.0544 min^{-1} and 0.016 min^{-1} for k_1 respectively, while Namasivayam and Sangeetha [24] reported k_2 value of 0.048 g mg^{-1} min^{-1}.

[INSERT FIG 3 HERE]

Thus it can be seen that the values obtained in this study compares favourably well with those obtained in other studies. To probe further into the rate of internal mass transfer, data was fitted to the intraparticle diffusion model (Fig. 3c). An excellent fit of the experimental data to the intraparticle diffusion model should show a strong linear relationship with the straight line passing through the origin. However, this is apparently not the case even though there is a linear relationship as suggested by the plots at the respective concentrations (Fig. 3c). This indicates that, whereas particle diffusion mechanism is involved, it may not be the rate-limiting mechanism. As can be deduced from Fig. 3c, increasing the phosphate concentration in the solution promoted the diffusion in the alum sludge particles and this resulted in an increase in the intraparticle diffusion rate. The rate constants as calculated from the regression equation increased from 0.0075 mg g^{-1} min^{-1} at 5 mg L^{-1} to 0.1795 mg g^{-1} min^{-1} at 60 mg L^{-1} indicating that more phosphate is adsorbed per gram.min at the higher P concentration. At this stage, it can be suggested that the adsorption of phosphate probably takes place via surface exchange reaction until the surface functional sites are fully occupied. Thereafter, the phosphate molecules diffuse into the pores of the alum sludge for further reactions. This has also been suggested as possible kinetic mechanism for the adsorption of P by water treatment residuals from recent studies [10]. They postulated that P may be initially adsorbed as an outer sphere complex or found in the diffuse ion swarm near individual particles.

To lend credence to this, results from this study further highlight the better linearity obtained at higher P concentration (R^2 = 0.62, 0.85, 0.96 and 0.90 for P concentration values of 5, 15, 30 and 60 mg L^{-1}). This suggests that intraparticle diffusion may be a predominant mechanism for P adsorption at high P concentration. It can be reasoned that the higher concentration provides a higher gradient which drives the ions into the pores. According to Walker et al. [28], the initial stage of the intraparticle diffusion represents external mass

transfer, followed by intraparticle diffusion into the macro, meso and micro-pore structure of the adsorbent. In this study, the plots obtained do suggest to some extent, the presence of intraparticle diffusion (pore diffusion), but it also indicates that it is not the only rate controlling step.

The calculated values of $\overline{D}$ obtained in this study at different initial P concentrations of 5, 15, 30 and 60 mg L^{-1} were 1.98×10^{-10}, 6.67×10^{-11}, 2.67×10^{-11}, and 2.22×10^{-11} cm^2 s^{-1}. According to Michelsen et al. [29], a $\overline{D}$ value of the order of 10^{-11} is indicative of intraparticle diffusion as the rate limiting step. Based on this, it can be suggested that intraparticle diffusion predominates at the high initial P values. Namasivayam and Sangeetha [24] in their study on P adsorption onto $ZnCl_2$ activated coir pith carbon reported $\overline{D}$ values in the order of 10^{-12} to 10^{-13} cm^2 s^{-1} and concluded that the P adsorption follows a pore diffusion process. Analysis of experimental data obtained in this study however suggests that such intraparticle (pore) diffusion predominates at high P concentrations.

3.3 Mass transfer and rate determining step

The experimental data were also well fitted to the mass transfer model (Fig. 4) with fairly and comparative low values of β_L obtained. The β_L values ranged from 1.7×10^{-6} to 1.8×10^{-8} and the values were found to decrease with increasing initial P concentration. The fairly low values of β_L obtained indicate a rapid transportation of the adsorbate from bulk to solid phase and it reflects the good efficiency of the adsorbent towards the adsorbate [30, 31]. The fitting of the experimental data to the model of Boyd and Reichenberg [17, 18] is shown in Fig. 5. The linear plots clearly indicate that at low concentration ($5 \leq P \leq 15$ mg P L^{-1}), the linearity of the plot deviates, whereas at higher concentrations, ($30 = P \leq 60$ mg P L^{-1}), the linearity is maintained.

[INSERT FIGURES 4 AND 5 HERE]

This phenomenon suggests the involvement of film diffusion and particle diffusion mechanisms as the rate controlling steps at lower and higher concentrations respectively. To further evaluate the data, the constant B was analysed. Values of B obtained compare favourably with those reported in literature [11] and also indicate that with increase in concentration, the rate of intraparticle diffusion also increases.

Conclusion

This study further demonstrates that alum sludge, a widely available by-product of water treatment plants can be used a cost-effective adsorbent for P in aqueous solutions. Analysis of adsorption data obtained in this study suggests that P adsorption takes place via surface exchange reaction until the surface functional sites are fully occupied. Thereafter, the P molecules diffuse into the pores of the alum sludge for further reactions. Higher rate constants were obtained at higher P concentrations indicating that more P is adsorbed per gram.min at higher concentration and the values of the mass transfer coefficient obtained indicate a rapid transportation of P onto the alum sludge. Wider, practical application of the results can include the use of the alum sludge to enhance phosphorus removal in treatment systems such as constructed and engineered wetlands.

Acknowledgement

Authors gratefully acknowledge the Irish Environmental Protection Agency for providing financial assistance for this study through the Environmental Technologies Scheme (project No. 2005-ET-MS-38-M3).

References

[1] K. Heal, P. Younger, K. Smith, S. Glendinning, P. Quinn, K. Dobbie, Novel use of Ochre from mine water treatment plants to reduce point and diffuse phosphorus pollution, Land Contam. Reclamation, 11 (2) (2003) 145-152

[2] EPA, Water Quality in Ireland 2004-2006, EPA (2008) Johnstown Castle, Co. Wexford, Ireland

[3] L. Johansson Westholm, Substrates for phosphorus removal-Potential benefits for on-site wastewater treatment? Water Res. 40 (1) (2006) 23–36.

[4] C. Vohla, M. Kõiva, H. J. Bavor, F. Chazarenc, Ü. Mander, Filter materials for phosphorus removal from wastewater in treatment wetlands—A review, Ecol. Eng. doi.10.1016/j.ecoleng.2009.08.003

[5] A.O. Babatunde, Y.Q. Zhao, Constructive approaches towards water treatment works sludge management: A review of beneficial reuses, Crit. Rev. Environ. Sci. Tech. 37(2) (2007) 129-164.

[6] A.O. Babatunde, Y.Q. Zhao, A.M. Burke, M.A. Morris, J.P. Hanrahan, Characterization of aluminium-based water treatment residual for potential phosphorus removal in engineered wetlands, Environ. Pollut. 157 (10) (2009) 2830–2836

[7] Y.Q. Zhao, X-H. Zhao, A.O. Babatunde, Use of dewatered alum sludge as main substrate in treatment reed bed receiving agricultural wastewater: Long-term trial', Bioresour. Technol. 100(2) (2009) 644-648.

[8] A.O. Babatunde, Y.Q. Zhao, X.H. Zhao, Alum sludge-based constructed wetland system for enhanced removal of P and OM from wastewater: Concept, design and performance analysis, Bioresour. Technol. 100(16) (2010) 6576-6579

[9] J.G. Kim, J.H. Kim, H. Moon, C. Chon, J.S. Ahn, Removal capacity of water plant alum sludge for phosphorus in aqueous solution, Chem. Speciation Bioavailability 14 (1-4) (2002) 67–73.

[10] J.A. Ippolito, K.A. Barbarick, D.M. Heil, J.P. Chandler, E.F. Redente, Phosphorus retention mechanisms of a water treatment residual, J. Environ. Qual. 32(5) 2003) 1857-1864

[11] V.K. Gupta, M. Gupta, S. Sharma, Process development for the removal of lead and chromium from aqueous solutions using red-mud-An aluminium industry waste, Water Res. 35(5) (2001) 1125- 1134

[12] Y.S. Ho, G. McKay, Pseudo-second-order model for sorption process, Proc. Biochem., 34(5) (1999) 451-465.

[13] W.J. Weber, J. Morris, Kinetics of adsorption on carbon from solution, J.Saint Eng Div Am Soc Civ Eng, 89 (1963) 31-60.

[14] F. Banat, S. Al-Asheh, L. Al-Makhadmeh, Evaluation of the use of raw and activated date pits as potential adsorbents for dye containing waters, Process Biochem, 39(2) (2003) 193-202.

[15] A. K. Bhattacharya, C. Venkobachar, Removal of cadmium (II) by low cost adsorbent. J Env Eng ASCE, 110 (1984) 110-122

[16] G. McKay, S.J. Allen, I.F. McConvey, M.S. Otterburn, Transport processes in the sorption of colored ions by peat particles, J. Colloid Interface Sci. 80(2) (1981) 323-339.

[17] G.E. Boyd, A.W. Adamstown, L.S. Meyers, The exchange adsorption of ions from aqueous solution by organic Zeolites. II. kinetics, J. Am. Chem. Soc, 69(11) (1947) 2836-2848.

[18] D. Reichenberg, Properties of ion exchange resins in relation to their structure III kinetics of exchange, J. Am. Chem. Soc., 75 (1953) 589-597

[19] V.K. Gupta, A. Mittal, L. Krishnan, V. Gajbe, Adsorption kinetics and column operations for the removal and recovery of malachite green from wastewater using bottom ash, Sep. Purif. Technol. 40(1) (2004) 87-96.
[20] Y. Yang, Y. Q. Zhao, A.O. Babatunde, L. Wang, Y.X. Ren, Y. Han, Characteristics and mechanisms of phosphate adsorption on dewatered alum sludge, Sep. Purif. Technol. 51(2) (2006) 193–200.
[21] M. Razali, Y.Q. Zhao, M. Bruen, Effectiveness of a drinking-water treatment sludge in removing different phosphorus species from aqueous solution, Sep. Purif. Technol. 55 (3) (2007) 300-306.
[22] K. Sakadevan, H.J. Bavor, Phosphate adsorption characteristics of soils, slags and zeolite to be used as substrates in constructed wetland systems, Water Res. 32 (2) (1998) 391–399.
[23] C.A Basar, Applicability of the various adsorption models of three dyes adsorption onto activated carbon prepared waste apricot, J. Hazard. Mater, 135(1-3) (2006) 232-241.
[24] C. Namasivayam, D. Sangeetha, Equilibrium and kinetic studies of adsorption of phosphate onto $ZnCl_2$ activated coir pith carbon, J. Colloid Interface Sci. 280(2) (2004) 359-365
[25] C. Namasivayam, K. Prathap, Recycling Fe (III)/Cr (III) hydroxide, an industrial solid waste for the removal of phosphate from water, J. Hazard. Mater. 123(1-3) (2005) 127-134.
[26] M. Ozacar, Contact time optimization of two-stage batch adsorber design using second-order kinetic model for the adsorption of phosphate onto alunite, J. Hazard. Mater. 137(1), (2006) 218-225.
[27] M. Ozacar, Equilibrium and kinetic modelling of adsorption of phosphorus on calcined alunite, Adsorption, 9(2) (2003) 125-132.
[28] G.M. Walker, L. Hansen, J-A. Hanna, S.J. Allen, Kinetics of a reactive dye adsorption onto dolomitic sorbents, Water Res. 37(9) (2003) 2081-2089.
[29] L.D. Michelsen, P.G. Gideon, E.G. Pace, L.H. Kutat, Removal of soluble mercury from wastewater by complexing techniques, Virgina Wat. Resources. Res.. Bull., No. 14(1975) 1-88
[30] A. Mittal, A. Malviya, D. Kaur, J. Mittal, L. Kurup, Studies on the adsorption kinetics and isotherms for the removal and recovery of methyl orange from wastewater using waste materials, J. Hazard Mater. 148(1-2) (2007) 229-240
[31] A. Mittal, J. Mittal, L. Kurup, Adsorption isotherms, kinetics and column operations for the removal of hazardous dye,Tartrazine from aqueous solutions using waste materials-Bottom Ash and De-Oiled Soya as adsorbents, J. Hazard. Mater. 136(3) (2006) 567-578.

Table(s)

Table 1 Adsorption isotherm model equations, corresponding linear forms and parameters obtained from linearization

Model	Equation	Linear form		Parameters obtained from linearization		
				pH 4	pH 7	pH 9
Langmuir	$q_e = \frac{Q_0 b C_e}{1 + b C_e}$	$\frac{C_e}{q_e} = \frac{a_L}{K_L} C_e + \frac{1}{K_L}$	Q_o (mg-P/g)	31.9	23.0	10.2
			b (L/mg)	0.027	0.025	0.024
			R^2	0.98	0.97	0.97
Freundlich	$q_e = K_F C_e^{1/n}$	$\log q_e = \log K_F + \frac{1}{n} \log C_e$	k_f (L/g)	0.67	0.53	0.41
			n	1.13	1.24	1.24
			R^2	0.91	0.93	0.88
D-R	$q_e = q_m e^{-k\varepsilon^2}$	$\ln q_e = \ln q_m - k\varepsilon^2$	q_m (mg-P/g)	5.23	3.32	2.69
			K (mol^2/kJ^2)	0.0011	0.0013	0.0016
			E (kJ/mol)	21.3	19.6	17.7
			R^2	0.84	0.81	0.65
Temkin	$q_e = \frac{RT}{b} \ln(k_T C_e)$	$q_e = B_1 \ln k_T + B_1 \ln C_e$	B_1	10.35	7.82	5.62
			k_T (L/mg)	0.93	0.82	0.82
			R^2	0.93	0.94	0.97
Frumkin	$\frac{\theta}{1-\theta} e^{-2a\theta} = KC_e$	$\log\left[\left(\frac{\theta}{1-\theta}\right)\frac{1}{C_e}\right] = \log K + 2a\theta$	a	1.27	0.62	1.04
			ln k	-1.32	-1.03	-1.03
			R^2	0.96	0.97	0.97
H-J	$\frac{1}{q_e^2} = \left(\frac{B}{A}\right) - \left(\frac{1}{A}\right) \log C_e$	$\frac{1}{q_e^2} = \left(\frac{B}{A}\right) - \left(\frac{1}{A}\right) \log C_e$	A	1.78	12.8	13.7
			B	1.52	1.82	2.1
			R^2	0.62	0.61	0.69

Figure captions

Fig. 1 SEM image of the dewatered alum sludge (using LEO 1530 VP, Leo Ltd, Germany)

Fig. 2 Adsorption plots for phosphate adsorption onto alum sludge at three different pH values using linearised forms of (a) Langmuir (b) Freundlich (c) D-R (d) Temkin (e) Frumkin and (f) Harkins – Jura model

Fig. 3 Sorption kinetics of P onto alum sludge at four different initial P concentrations using (a) first (b) second order and (c) intraparticle diffusion models (initial solution pH = 7)

Fig. 4 Plot of Log A^* versus time for the mass transfer of phosphorus onto alum sludge at different initial concentrations. $A^* = \left[\frac{C_t}{C_O} - \frac{1}{1+mk}\right]$ (initial solution pH = 7)

Fig. 5 Plot of B_t versus time for the adsorption of phosphorus onto alum sludge at different initial concentrations (initial solution pH = 7)

Figure 1

Figure 2

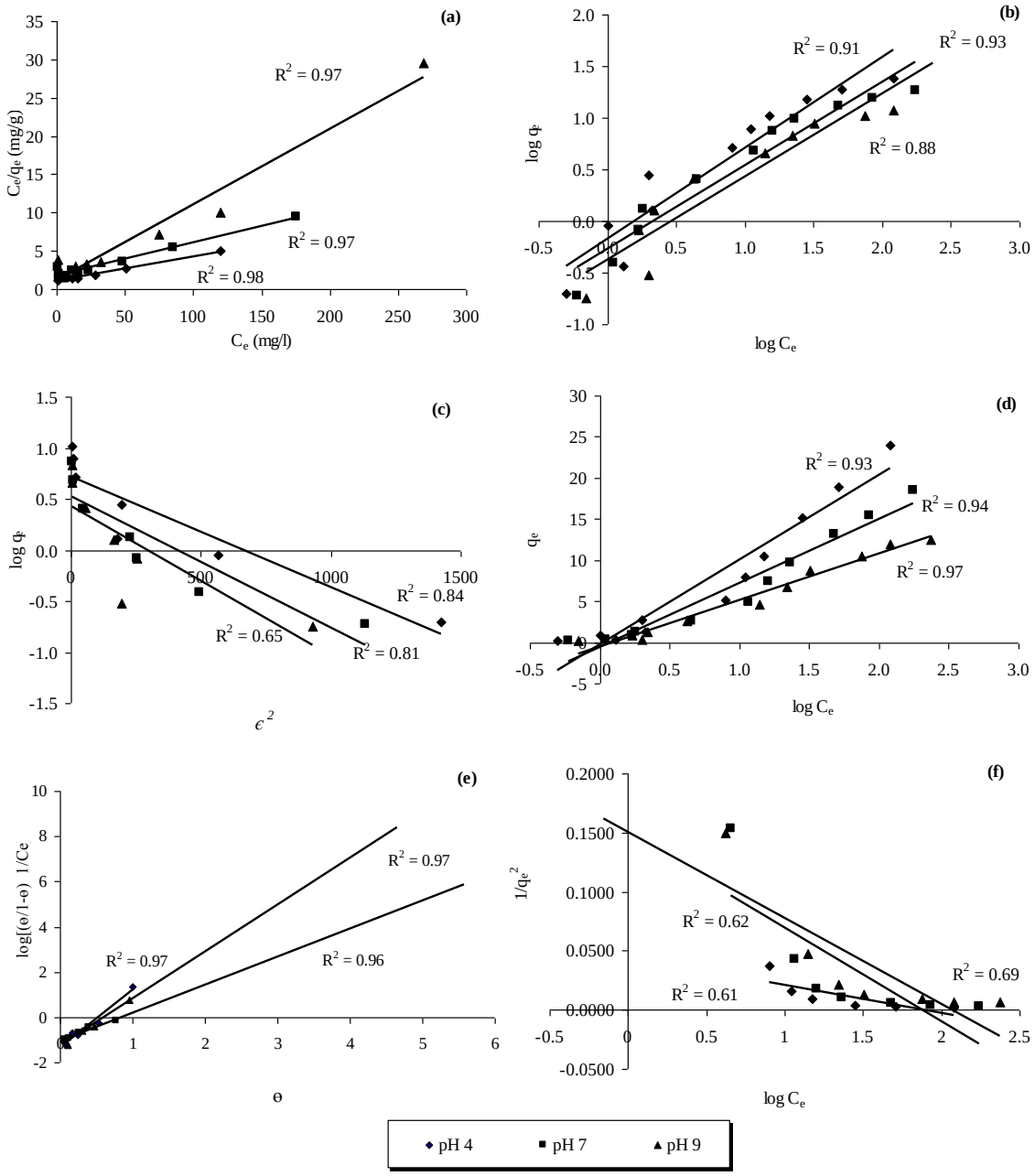

Fig. 2

Figure 3

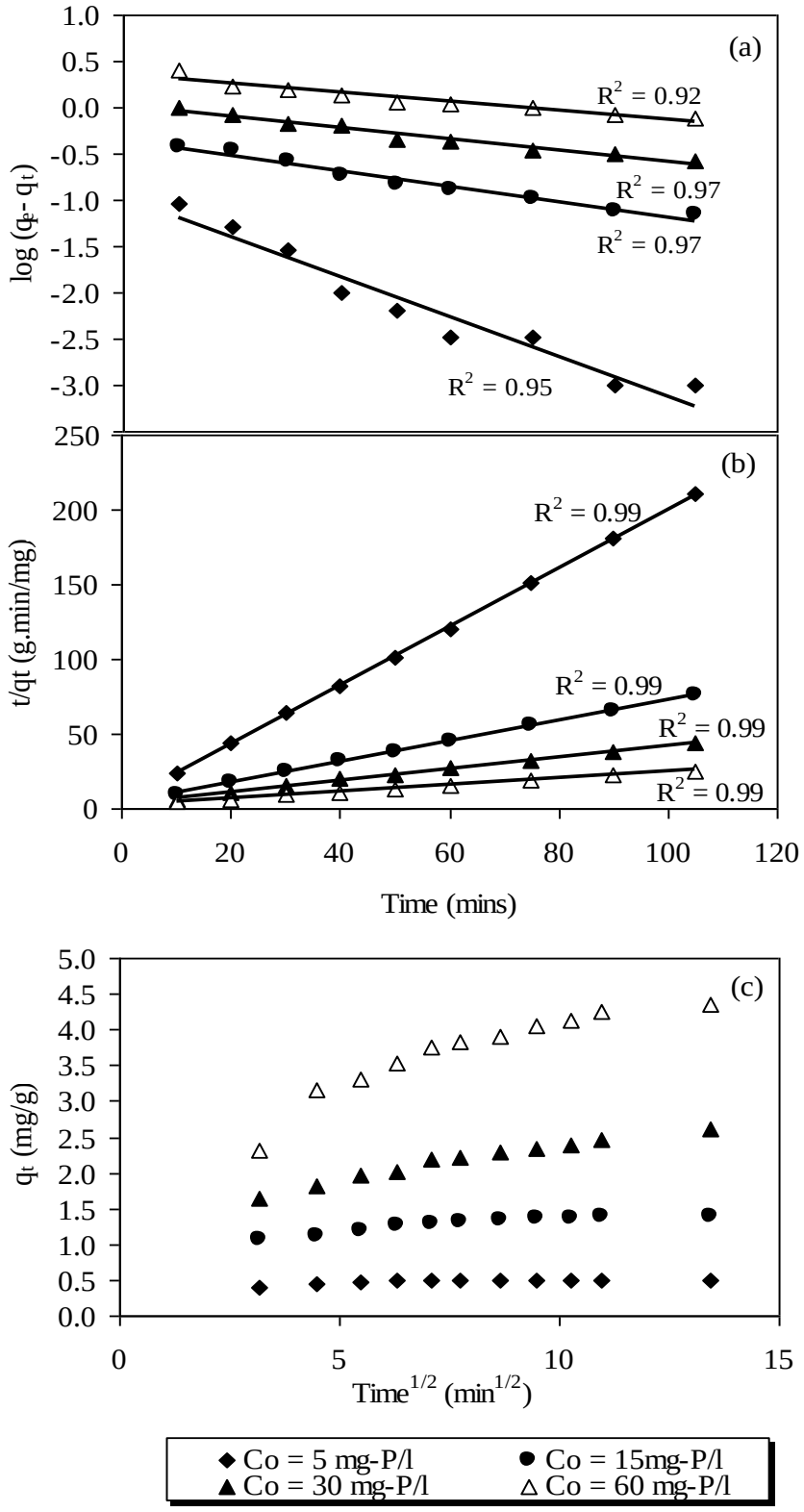

Fig. 3

Figure 4

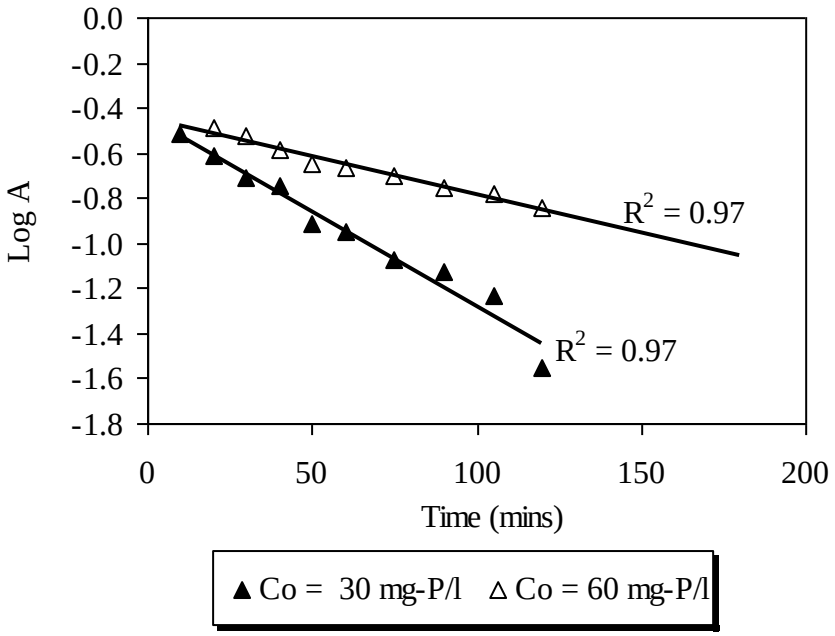

Fig. 4

Figure 5

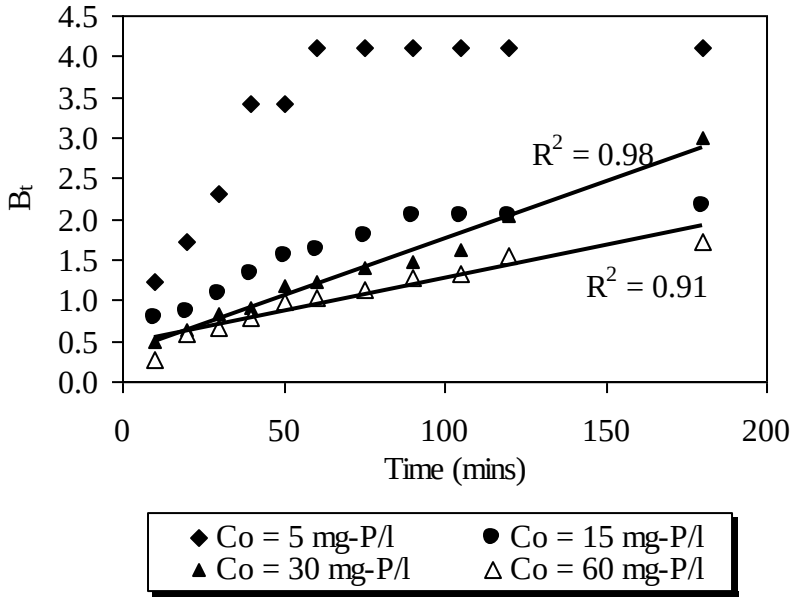

Fig. 5